ELSEVIER

Journal of Magnetism and Magnetic Materials 159 (1996) 125–134

journal of magnetism and magnetic materials

Relaxation of thermoremanent magnetization in the spin-glass phase of itinerant magnetic Fe_xTiS_2

Y. Hara, H. Negishi, M. Sasaki, M. Inoue *

Department of Materials Science, Faculty of Science, Hiroshima University, Higashi-Hiroshima 739, Japan

Received 29 August 1995; revised 1 November 1995

Abstract

Time decays of the thermoremanent magnetization (TRM) in the spin-glass phase of Fe_xTiS_2 ($x = 0.20$, $T_g = 41$ K) have been measured using the anomalous Hall effect over the time range 10^{-2}–10^4 s with waiting time $t_w = 180$–18000 s at temperatures T below $T/T_g \sim 0.7$. After the cooling field H_{FC} (0.01–0.14 T) is switched off, the Hall resistivity (or TRM), within a short time span, follows a power law of the form $\rho_H(t) = At^{-m}$ (A is a constant), where the magnetic field and temperature-dependent exponent m are expressed in a universal form, $m = D\xi^{\gamma}$, with the parameter of 'relative relaxed magnetization' (RRM) ξ. The decay profiles over the wide time range are analyzed using the existing 'domain theory' with some modifications of the theoretical expressions. With the evaluated parameters, the equilibrium relaxation spectra, overlap lengths, and time-dependent maximum relaxation times that characterize the domain growth and the dynamical properties in this material are discussed.

Keywords: Relaxation; Spin glass; Itinerant magnetism; Domain theory

1. Introduction

With regard to the dynamical treatment of spin-glass (SG) systems, there are two different viewpoints. One is the mean-field approach of Sherrington–Kirkpatrick (SK) and its replica symmetry solution by Parisi, giving an infinite number of quasi-equilibrium states which are hierarchically organized in phase space – 'hierarchical kinetic model'. This model has been shown to be valid for relaxation of thermoremanent magnetization (TRM) in insulating SG of $CdCr_{1.7}In_{0.3}S_4$ [1,2] and dilute Ag:Mn alloy (2.6 at% Mn) [3]; from numerical and theoretical studies, Newman and Stein have pointed out that the Parisi solution to the SK model cannot apply to short-range spin glasses [4]. The other treatment is a phenomenological approach based on the existence of a distribution of droplets [5] or dynamical domains [6], which has been applied to the interpretation of the aging and time decay of TRM for various SG systems, such as $CdCr_{1.7}In_{0.3}S_4$ [6] and Cu (10 at% Mn) [7]. The former model is concerned with, in particular, the temperature cycle in the aging effect of TRM, while the latter deals with its time dependence, which shows the existence of a clear crossover from dynamical processes characterized by length scales smaller than the already achieved domain size (quasi-equilibrium regime) to processes on larger time scales dominated by the continuation of domain

* Corresponding author. Fax: +81-824-240721; email: inoue@aso.sci.hiroshima-u.ac.jp.

SSDI 0304-8853(95)00947-7

growth through the movement of domain walls across the system (non-equilibrium regime). In the latter picture, aging is a manifestation of slow domain growth below glass temperature, where after a certain waiting time t_w a characteristic domain size is reached. However, the time dependence of the domain size $s(t)$ is treated differently; Fisher and Huse (FH) [5] suggest a logarithmic dependence $s(t) \propto (\log t)^{1/\psi}$ from an activated dynamics scenario, while Koper and Hilhorst (KH) [6] assume the power law $s(t) \propto t^p$. In the present study, we shall discuss our results within the framework of the realistic KH domain theory.

In contrast to magnetic measurements for various localized systems, we have studied the dynamics of zero-field-cooled (ZFC) isothermal remanent magnetization (IRM) and field-cooled TRM for SG and cluster-glass (CG) phases of itinerant magnetic systems of the intercalation compound Fe_xTiS_2 using the transport method [8,9], since this material shows an anomalous Hall effect, in which the Hall resistivity ρ_H can be expressed in the well known form $\rho_H = R_0 H + 4\pi R_s M(H)$, where R_0 and R_s are the normal and extraordinary Hall coefficients, respectively, and $M(H)$ the magnetization at magnetic field H. When the applied field H is turned off, the Hall resistivity $\rho_H(t)$ is proportional to the remanent magnetization $M(t)$ at time t, as $\rho_H(t) = 4\pi R_s M(t)$. For the IRM case, it decays with time obeying a power law of the form

$$\rho_H(t) = At^{-m}, \tag{1}$$

while for TRM this is valid only in a short time span. In addition, the exponent m, which depends on both magnetic field and temperature, is expressed by the universal relationship

$$mT^{\alpha} = C\phi^{\beta} \quad (\alpha \text{ and } \beta \text{ are constants}), \tag{2}$$

with the parameter of 'relative relaxed magnetization' (RRM) ϕ, defined as $\phi = 1 - M(0)/M(H_p) = 1 - \rho_H(0)/[\rho_H(H_p) - R_0 H_p]$, where $M(0)$ and $M(H_p)$ are the magnetization at $t = 0$ and $H = H_p$ (external pulsed field intensity), respectively. This relation is satisfied for both SG and CG phases [8]. For TRM, a similar universal relation is found to hold for the case of the CG phase

$$m = D\xi, \tag{3}$$

where D is a dimensionless constant and ξ another RRM parameter, defined by $\xi = 1 - M(0)/M^{FC}(T \to 0)$ [9]. Here, $M(0)$ is the magnetization at time $t = 0$ when the cooling field H_{FC} is switched off and $M_{FC}(T \to 0)$ is the value extrapolated to absolute zero of the magnetization at temperature T and cooling-field intensity H_{FC}.

The present purpose is two-fold; firstly, an analysis of the time decay profiles of TRM (including the effect of the waiting time on aging) to obtain some dynamical parameters for the SG phase of Fe_xTiS_2 ($x = 0.20$) according to the realistic 'domain theory' developed by Koper and Hilhorst [6], and secondly the examination of the validity of the universal relation such as in Eq. (3) for TRM.

2. Experimental

Single crystals of $Fe_{0.20}TiS_2$ (SG phase, glass temperature $T_g = 41$ K) were grown by a chemical vapor transport method using I_2 as transport gas, as done previously. Ohmic contacts to the sample with a six-probe for Hall effect measurements were made by soldering indium metal. The transport measurements were performed using a conventional dc potentiometric method in the same experimental setup as employed in earlier work [9]. For TRM measurements, a magnetic field with intensity $H_{FC} = 0.01$–0.14 T for field cooling was applied to the sample at about 60 K ($T/T_g \sim 1.5$) and then the temperature was lowered at a constant rate (1 K/min) to the working temperature T. After a waiting time of $t_w = 180$, 1800 or 18000 s the field was switched off and the time decay of the Hall voltage was subsequently recorded using a digital storage oscilloscope (in the time span 0–50 ms) or a nanovoltmeter (10^{-1}–10^4 s). After the measurements the sample was warmed to 60 K in zero field and then the reversed magnetic field was applied, followed by the above procedure to exclude any spurious contributions from misaligned contacts and thermoelectromotive force generated at the In/Fe_xTiS_2 interface against the Hall voltages.

3. Results

Fig. 1 shows typical time variations at 16.8 K of (a) the cooling field $H_{FC} = 0.14$ T and (b) Hall

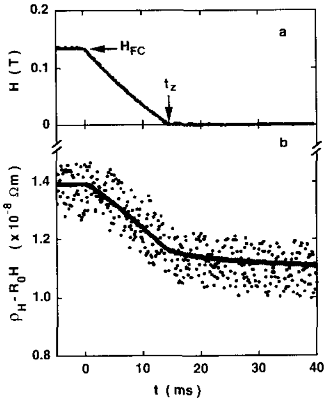

Fig. 1. Typical time variation at 16.8 K of (a) the external magnetic field from cooling field H_{FC} (initially at 0.14 T) and (b) the Hall resistivity ($\rho_H - R_0 H$) corresponding to magnetization $M(t)$. The solid curve in (b) was calculated using Eq. (13) and Eq. (14) with the best-fit parameters $m = 0.027$, $t_0 = 7 \times 10^{-6}$ s, $pz = 0.9$, $t_2^{pz}/t_1 = 0.0075$ s^{pz-1} and $t_{\Delta H} = 40$ s (see text).

resistivity, $\rho_H - R_0 H$, where the time is set to zero when the cooling field begins to decrease; the normal Hall coefficient was determined to be $R_0 = -7.4 \times 10^{-9}$ m^3/C, which is independent of temperature. The applied magnetic field H is decreased from the cooling field $H_{FC} = 0.14$ T at a constant rate $\delta H = 10$ T/s and vanishes at time $t_z = H_{FC}/\delta H = 14$ ms, as indicated by the arrows. We should note that t_z is very short compared with the waiting time $t_w = 180$–$18\,000$ s and the time span of relaxation measurements (10^4 s). As the magnetic field is decreased to zero, the Hall resistivity decays with time from 1.4×10^{-8} to 1.15×10^{-8} Ω m at time t_z, and in zero field it continues to relax slowly. In our previous report for the CG phase [9], the time origin was set to zero when H attained zero, while in the present study the above set time is used in order to calculate the time dependence of the Hall resistivity (or TRM) based on the domain theory; the solid curve in Fig. 1b was calculated using Eq. (13) and Eq. (14) with the best-fit parameters (see later).

Similar measurements were carried out at various cooling fields and temperatures. Fig. 2 plots the values of the Hall resistivity ($\rho_H^{FC} - R_0 H_{FC}$) ($\propto M^{FC}$) at H_{FC} (solid circles) and the Hall resistivity $\rho_H(t_z)$ at time t_z, where $H = 0$ (open squares), versus (a) the cooling-field intensity H_{FC} at a fixed temperature of 16.8 K and (b) versus temperature at a fixed cooling field of $H_{FC} = 0.14$ T. The values of ($\rho_H^{FC} - R_0 H_{FC}$) and $\rho_H(t_z)$ increase nonlinearly with H_{FC}, corresponding to the magnetization curve at H_{FC} and the remanent curve at time t_z. The temperature dependence of ($\rho_H^{FC} - R_0 H_{FC}$) is very small in the temperature range measured, 7.8–29.3 K; it will

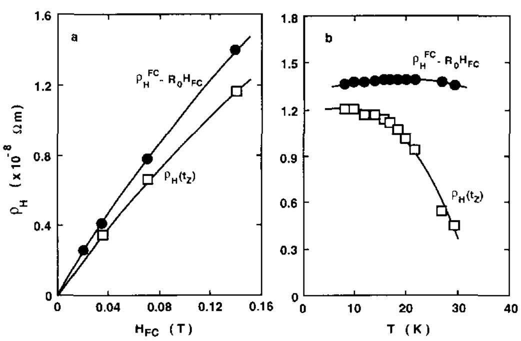

Fig. 2. Variation of the Hall resistivity ($\rho_H^{FC} - R_0 H_{FC}$) at H_{FC} (●) and the Hall resistivity $\rho_H(t_z)$ at time t_z (□) with (a) the cooling field H_{FC} at a fixed temperature of 16.8 K and (b) with temperature at a fixed cooling field of $H_{FC} = 0.14$ T.

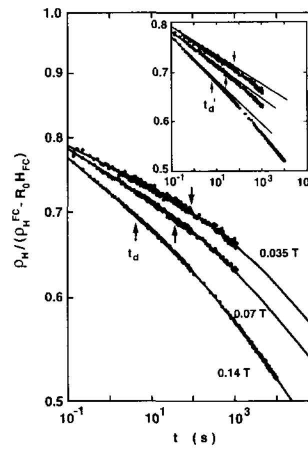

Fig. 3. Time decay of the Hall resistivities ρ_H at 16.8 K with $t_w = 1800$ s under various fields H_{FC}, normalized by ($\rho_H^{FC} - R_0 H_{FC}$) at H_{FC} in log–log plots. Arrows mark the deviation time t_d, above which the experimental points deviate from the power law of Eq. (1). The solid curves were calculated using Eq. (14) with the magnetic field-independent parameters $pz = 0.9$ and $t_2^{pz}/t_1 = 0.0075$ s^{pz-1}, and the field-dependent parameters m, t_0 and $t_{\Delta H}$ (see text). The inset shows semi-logarithmic plots of the same data, where arrows mark the deviation time t_d' above which the data points deviate from the logarithmic form, $\rho_H(t) = C - D \log t$.

decrease drastically as the temperature is raised toward the glass temperature $T_g = 41$ K. On the other hand, $\rho_H(t_z)$ shows a profound temperature variation above 20 K, where the value of $\rho_H(t_z)$ (magnetization at time t_z) is decreased to nearly a half of $(\rho_H^{FC} - R_0 H_{FC})$ (magnetization at the start, $t = 0$).

Fig. 3 illustrates in log–log plots the time decay of the Hall resistivity ρ_H after the cooling field is switched off with waiting time $t_w = 1800$ s at 16.8 K under different field intensities H_{FC}, where ρ_H is normalized by the initial value $(\rho_H^{FC} - R_0 H_{FC})$. The experimental points lie on straight lines (the power law $\rho_H(t) = At^{-m}$ of Eq. (1), $m = 0.018$–0.027) up to the lapse time t_d marked by arrows, beyond which the deviations from Eq. (1) become appreciable; here, we define the deviation time t_d as the time at which the deviations begin to increase more than a quarter of the mean square errors, as done for a SG material of $Eu_{0.4}Sr_{0.6}S$ [10]. Although not shown here, only at 26.8 K and $H_{FC} = 0.14$ T is the power law satisfied over the entire time range up to 10^4 s, which is similar to that found for field-cooled TRM data of the CG phase of Fe_xTiS_2 ($x = 1/4$) obtained at $H_{FC} = 0.14$ T and 27.4 K [9]. We have also found that these decay curves are independent of waiting time $t_w = 180$–18000 s under the experimental conditions of $H_{FC} = 0.01$–0.14 T and temperatures $T = 7.8$–29.3 K, which we shall discuss later in terms of the 'overlap length' introduced by Bray and Moore [12]. Furthermore, these curves can also be fitted by a logarithmic dependence of the form $\rho_H(t) = C - D \log t$ (C and D are constants), as depicted in the inset of Fig. 3 plotted on a semi-logarithmic scale, where the arrows mark the deviation time t_d' in each curve (t_d' is almost the same as t_d); such a logarithmic dependence is valid for $m \ll 1$, as already discussed for IRM studies [11]. In the present work, we have employed the power law of Eq. (1) to discuss our results within the framework of the KH domain theory.

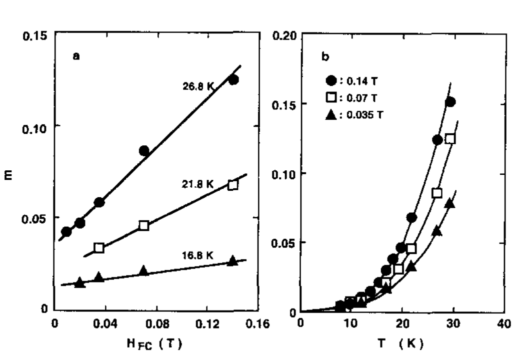

Fig. 4. Variation of the exponent m with (a) the cooling field H_{FC} at various temperatures and (b) with temperature at different cooling fields.

Fig. 4 shows the exponent m for TRM plotted versus (a) the cooling field at different temperatures and (b) versus temperature at different field intensities H_{FC}. The exponent m increases linearly with increasing cooling field and also increases drastically as the temperature is increased toward T_g. This behavior for SG is nearly the same as that for CG [9].

4. Discussion

4.1. Domain theory for the time decay of TRM

We shall now consider the observed decay curves for TRM over the whole time range where deviations from the power law occur. Since our results show the power law in a short time region, we have analyzed them using the KH domain theory, employing the power law for the equilibrium relaxation function [6] rather than the FH law [5]. However, Koper and Hilhorst derived theoretical expressions with an idealized stepwise form for switching off an external cooling field H_{FC}, whereas in our actual experiments it decreased at a constant rate δH to zero within time t_z. Thus, we need some modifications of their expressions, as described below.

According to the KH model, the magnetization is expressed by assuming that linear response theory is valid for relaxation of SG

$$M(t) = \Delta M(t) + N\chi_{eq} H(t)$$
$$= -N\chi_{eq} \int_0^t dt' \, R(t,t') \dot{H}(t') + N\chi_{eq} H(t), \quad (4)$$

where $\Delta M(t)$ is the excess magnetization, N the number of spins in the sample, and χ_{eq} the equilibrium dc susceptibility in zero field. Based on experimental data [13] and Monte Carlo simulations [14], the relaxation function $R(t,t')$ is written as

$$R(t,t') = R_{eq}(t-t')F(t,t'). \tag{5}$$

In thermal equilibrium, $R_{eq}(t-t')$ is given by

$$R_{eq}(t-t') = \left[1 + (t-t')/t_0\right]^{-m}, \tag{6}$$

where t_0 specifies the minimum relaxation time in the equilibrium relaxation spectrum, as discussed in Section 4.2. A plausible choice for $F(t,t')$ is a cutoff reflecting deviations from equilibrium, $F(t,t') = \exp[-(t-t')/\tau_{max}(s)]$, where $\tau_{max}(s)$ is the maximum relaxation time in the relaxation spectrum of a size s domain, and a plausible generalization of $F(t,t')$ using the time-dependent domain size $s(t'')$ $(t' < t'' < t)$ gives

$$F(t,t';[s(t'')]) = \exp\left\{-\int_{t'}^{t} dt''/\tau_{max}[s(t'')]\right\}. \tag{7}$$

Due to the spin coherence within a domain, $\tau_{max}(s)$ is assumed to be a function of domain size with typical spin spacing a

$$\tau_{max}(s) \cong t_1(s/a)^z, \tag{8}$$

where t_1 is the microscopic time constant and z a dynamical parameter.

Furthermore, Bray and Moore [12] predicted that, during waiting time t_w, the domain size $s(t)$ cannot grow larger than an 'overlap length' $l_{\Delta H}$ for a given magnetic field jump ΔH (in our case H_{FC}), which is written as $l_{\Delta H} \sim |\Delta H|^{-2/(d-2y)}$ with the dimension of the system d and constant y. Taking into account the interplay between $s(t)$ and $l_{\Delta H}$, the KH model considers the following two cases: for a small field jump, $s(t_w) < l_{\Delta H}$, the domain size $s(t)$ increases as a power of time

$$s(t) \cong a\left[(t_w + t)/t_2\right]^p, \tag{9}$$

where t_2 is the microscopic time and p another dynamical parameter. For a large field jump, where the linear size of domains reaches its upper limit $l_{\Delta H}$ during waiting time t_w, $s(t_z) = l_{\Delta H}$, and thus $s(t)$, is written as, for $t > t_z$,

$$s(t) \cong a\left[(l_{\Delta H}/a)^{1/p} + (t - t_z)/t_2\right]^p. \tag{9'}$$

The waiting time t_w does not enter into this expression, indicating that it does not affect the domain size after switching off the external field. Since there is no t_w dependence of the observed decay curves, we use Eq. (9′) for the time dependence of the domain size. In addition, a time $t_{\Delta H}$ is defined, during which the domain is growing to a size of $l_{\Delta H}$

$$t_{\Delta H} = t_2\left[(l_{\Delta H}/a)\right]^{1/p} \sim |\Delta H|^{-2/[(d-2y)p]}. \tag{10}$$

With this quantity and using Eq. (8) and Eq. (9′), the maximum relaxation time is given by

$$\tau_{max}(t) = (t_{\Delta H} + t - t_z)^{pz}(t_2^{pz}/t_1)^{-1}. \tag{11}$$

The time decay of TRM can be calculated using the above expressions. Taking into account the time-dependent magnetic field change at constant rate δH in our case, not stepwise as in the KH model, we express the time variation of the magnetic field, with $t_z = H_{FC}/\delta H$, as

$$\begin{aligned} H(t) &= H_{FC} - t\delta H \text{ for } 0 \le t \le t_z, \\ &= 0 \text{ for } t > t_z. \end{aligned} \tag{12}$$

In the time region $t \le t_z$ we may take $F(t,t') = 1$, since $t - t' \ll \tau_{max}(s)$, and we obtain

$$\begin{aligned} M(t) &= N\chi_{eq}\delta H\left[-t_0/(-m+1)\right] \\ &\quad \times \left[1 - (1 + t/t_0)^{-m+1}\right] \\ &\quad + N\chi_{eq}(H_{FC} - t\delta H). \end{aligned} \tag{13}$$

On the other hand, in the case of $t > t_z$, $F(t,t') \neq 1$, yielding

$$\begin{aligned} M(t) &= \Delta M(t) \\ &= N\chi_{eq}\delta H\int_0^{t_z} dt'\left[1 + (t-t')/t_0\right]^{-m} \\ &\quad \times \exp\Big\{\Big[(t_{\Delta H} + t - t_z)^{1-pz} \\ &\quad - (t_{\Delta H} + t' - t_z)^{1-pz}\Big]t_2^{pz}/\left[t_1(1-pz)\right]\Big\}. \end{aligned} \tag{14}$$

The above integration cannot be carried out analytically and therefore we have made a numerical integration to calculate TRM. For the numerical calculations of Eq. (13) and Eq. (14), we have assumed the following conditions for the fitting parameters: (i) we take the observed exponent m, (ii) pz is a universal constant independent of temperature and magnetic field, (iii) the ratio t_2^{pz}/t_1 is a function of temperature alone, and (iv) both t_0 and $t_{\Delta H}$ depend on temperature and magnetic field.

As an example, the solid line in Fig. 1 shows the calculated curve of the Hall resistivity (or TRM) using Eq. (13) and Eq. (14) with the best-fit values of $m = 0.027$, $t_0 = 7 \times 10^{-6}$ s, $pz = 0.9$, $t_2^{pz}/t_1 = 0.0075$ s^{pz-1}, and $t_{\Delta H} = 40$ s in the time range $t = 0$–40 ms, where the cooling field is decreasing at constant rate 10 T/s, in satisfactory agreement with observation. Furthermore, we have performed numerical calculations of the overall time decay of TRM under various conditions (temperatures and cooling-field intensities) using Eq. (14) to obtain reasonable agreement with experiments, as shown by the solid curves in Fig. 3; the parameters used for the calculations are the field-independent ($pz = 0.9$, $t_2^{pz}/t_1 = 0.0075$ s^{pz-1}) and the field-dependent parameters ($m = 0.018$, 0.022 and 0.027, $t_0 = 9 \times 10^{-8}$, 7×10^{-7} and 7×10^{-6} s, $t_{\Delta H} = 350$, 130 and 40 s for $H_{FC} = 0.035$, 0.07 and 0.14 T, respectively). We shall discuss the obtained dynamical parameters below.

4.2. Equilibrium relaxation – the power law

We shall now focus on the dynamical parameters t_0 and exponent m of the equilibrium relaxation function $R_{eq}(t - t')$ in Eq. (6). For a system with a distribution function of relaxation time τ, $P(\tau)$, the equilibrium relaxation function is given by $R_{eq}(t - t') = \int d\tau\, P(\tau)\exp[(t - t')/\tau]$. Using an inverse

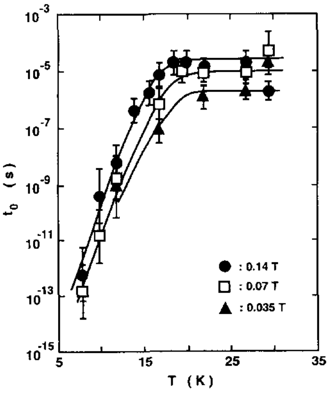

Fig. 5. The best-fit values of the minimum relaxation time t_0 at different cooling fields H_{FC} plotted versus temperature.

Laplace transform, we can obtain $P(\tau)$ corresponding to $R_{eq}(t - t')$ with the power law form of Eq. (6)

$$P(\tau) = [t_0/\Gamma(m)](\tau/t_0)^{-(m+1)}\exp(-t_0/\tau), \tag{15}$$

where $\Gamma(m)$ is a gamma function of m. In terms of the relaxation spectrum $Q(\tau)$, which is defined by $R_{eq}(t - t') = \int d(\ln\tau)\, Q(\tau)\exp[(t - t')/\tau]$, we obtain

$$Q(\tau) = [1/\Gamma(m)](\tau/t_0)^{-m}\exp(-t_0/\tau). \tag{15'}$$

From the form of Eq. (15′), we see that t_0 is the minimum relaxation time and m characterizes the distribution intensity and width of the relaxation spectrum.

The best-fit parameters t_0 obtained at different magnetic fields are plotted against temperature in Fig. 5. With increasing temperature, the values of t_0 increase appreciably from 10^{-13} to 10^{-12} s at around 8 K and tend to saturate above 18 K at values as high as 10^{-6}–10^{-4} s. We also note that t_0 increases with the cooling field H_{FC}. The magnitude of t_0 for our system is comparable to those for the insulating SG of $CdCr_{1.7}In_{0.3}S_4$ ($t_0 \sim 10^{-15}$ s) [6] and $Fe_{0.5}Mn_{0.5}TiO_3$ ($t_0 = 10^{-6}$–10^{-5} s estimated from the reported decay curves) [15].

As shown above (Figs. 4 and 5), both exponent m and minimum relaxation time t_0 depend strongly on cooling-field intensity H_{FC} and temperature. We then examined the validity of the universal relation between exponent m and the RRM parameter ϕ or ξ for the present SG phase; RRM parameters are defined by $\phi = 1 - M(t_z)/M^{FC}(T)$ and $\xi = 1 - M(t_z)/M^{FC}(T \to 0)$, where the magnetization at t_z, $M(t_z)$, is normalized by the value $M^{FC}(T)$ at T and that at absolute zero [denoted by $M^{FC}(T \to 0)$], respectively [8,9]. Fig. 6a plots the values of m versus ξ on a logarithmic scale; similar results are obtained for the plot of m versus ϕ, not shown here. We see that the experimental points lie on a single line with two different slopes above and below the characteristic point $\xi_C = 0.21$ marked by the arrow, which is well described by the expression

$$m = D\xi^{\gamma}, \tag{16}$$

where the best-fit parameters are determined to be $D = 0.30$ and $\gamma = 1.4$ for $\xi > \xi_C$ and $D = 2.6$ and $\gamma = 2.8$ for $\xi < \xi_C$. Thus Eq. (16) is regarded as a general expression for characterizing the dynamics of TRM in the short time range less than t_d for both

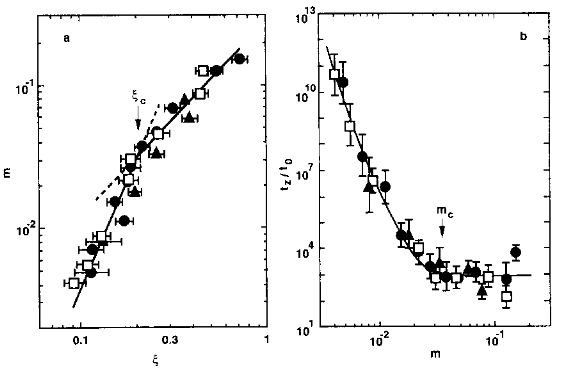

Fig. 6. (a) The exponent m plotted versus ξ, whose relation can be expressed in the form of Eq. (16) (see text). (b) The values of t_z/t_0 plotted versus m; symbols are the same as those in Fig. 5. Arrows mark the characteristic values of $\xi_C = 0.21$ and $m_C = 0.033$.

SG and CG of our magnetic material and ξ is a good parameter to describe the freezing state of SG and CG phases. We note that the γ value for SG ($\gamma = 1.4$ and 2.8) is larger than that for CG ($\gamma = 1.0$), which indicates that the dependence of m on ξ is much stronger in the former case than in the latter.

Now the RRM parameter ξ can be expressed using the dynamical parameters m and t_0, as given below. The magnetizations in ξ are written as $M^{FC}(T \to 0) = N\chi_{eq}(T \to 0)H_{FC}$ and $M(t_z) = N\chi_{eq}(T)\delta H[-t_0/(-m+1)][1-(1+t_z/t_0)^{-m+1}] \sim N\chi_{eq}(T)H_{FC}(t_z/t_0)^{-m}/(-m+1)$, thus ξ is rewritten as

$$\xi = 1 - M(t_z)/M^{FC}(T \to 0)$$
$$\sim 1 - \left[\chi_{eq}(T)/\chi_{eq}(T \to 0)\right] \times (t_z/t_0)^{-m}/(-m+1). \qquad (17)$$

Since $\chi_{eq}(T)/\chi_{eq}(T \to 0) \sim 1$ for general SG cases, including our results (see Fig. 2b), we obtain the simple form

$$\xi \sim 1 - (t_z/t_0)^{-m}/(-m+1). \qquad (17')$$

The values of t_z/t_0 are plotted versus m in Fig. 6b. With increasing m, t_z/t_0 decreases and becomes nearly constant above $m_C = 0.033$, marked by the arrow, which corresponds to the characteristic value $\xi_C = 0.21$ which represents the turning point where the minimum relaxation time t_0 (or t_z/t_0) depends on the temperature or not.

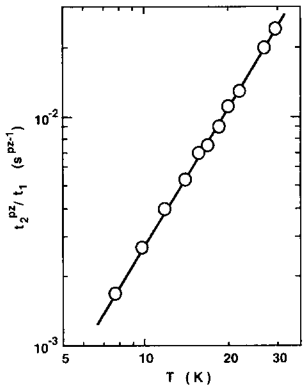

Fig. 7. The best-fit values of t_2^{pz}/t_1 plotted versus temperature on a logarithmic scale, which follow a single line, expressed as $t_2^{pz}/t_1 = 2.8 \times 10^{-5}T^2$.

4.3. Nonequilibrium relaxation

In nonequilibrium relaxation, the maximum relaxation time $\tau_{max}(t)$ $[=(t_{\Delta H} + t - t_z)^{pz}(t_2^{pz}/t_1)^{-1}]$ in Eq. (11) is an important quantity that characterizes the upper cutoff in the relaxation spectra of time-dependent domains. Fig. 7 plots the best-fit values of t_2^{pz}/t_1 versus temperature on a logarithmic scale, which follow a single line, as $t_2^{pz}/t_1 = 2.8 \times 10^{-5}T^2$. Fig. 8a shows the values of $t_{\Delta H}$, which characterizes the overlap length $l_{\Delta H}$, at different temperatures plotted versus cooling field H_{FC} on a logarithmic scale, where one can see that the experimental points lie on single lines at fixed temperatures, whose

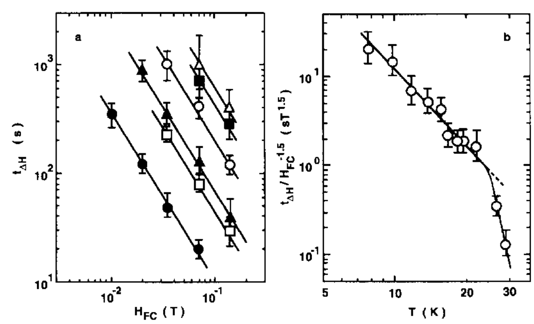

Fig. 8. (a) The best-fit values of $t_{\Delta H}$ at different temperatures plotted versus the cooling field H_{FC} on a logarithmic scale; symbols from open triangles to solid circles correspond to temperatures of 7.8, 9.8, 11.8, 16.8, 21.8 and 26.8 K, respectively. The slope of each line is equal to -1.5, which corresponds to $-2/[(d-2y)p]$ in Eq. (10). (b) The values of $t_{\Delta H}/H_{FC}^{-1.5}$ plotted versus temperature.

slopes are all equal to -1.5, or $t_{\Delta H} \sim H_{FC}^{-1.5}$. In order to see the temperature dependence of $t_{\Delta H}$, in Fig. 8b we illustrate the values of $t_{\Delta H}/H_{FC}^{-1.5}$ versus temperature in log–log plots. As the temperature is increased, the experimental points decrease following a straight line up to a temperature of about 20–25 K ($\cong T_g/2$), as $t_{\Delta H}/H_{FC}^{-1.5} = 1.2 \times 10^4 T^{-3}$, above which they show a steep decrease; such drastic temperature variations are also found in other quantities, such as $\rho_H(t_z)$ (Fig. 2b) and m (Fig. 4b). We should note that the ratio $t_2^{p_z}/t_1$ exhibits no drastic variation around that temperature (Fig. 7), while the value of $t_{\Delta H}$ or t_2 [see Eq. (10)] changes appreciably, which means that the time constant t_1 is reduced markedly above 20–25 K. These results indicate that thermal fluctuations in spin-glass systems become appreciable above this temperature.

From Figs. 7 and 8, we obtain $\tau_{max}(t) = 3.6 \times 10^4 T^{-2}(1.2 \times 10^4 H_{FC}^{-1.5} T^{-3} + t - t_z)^{0.9}$ for the maximum relaxation time at low temperatures below 20–25 K. The typical temperature dependence of the maximum relaxation time $\tau_{max}(t)$ for $H_{FC} = 0.14$ T at different times ($t = t_z$, 10^2, 10^3 and 10^4 s) is shown in Fig. 9 on a logarithmic scale; the curves at $t = t_z$ (the time when the external field is reduced to zero) and 10^4 s follow a straight line, but those at 10^2 and 10^3 s do not lie on a straight line. We see that $\tau_{max}(t)$ increases with time t, which indicates that the domain size in the SG system grows as time laps. Although not shown here, we also found that, at fixed temperature, $\tau_{max}(t)$ at $t = t_z$ depends strongly on the cooling field as $H_{FC}^{-1.35}$, but it becomes independent of H_{FC} for $t \gg t_z$.

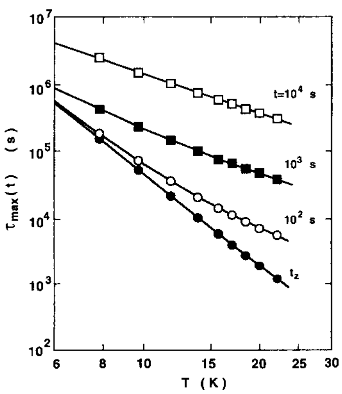

Fig. 9. The calculated values of maximum relaxation time $\tau_{max}(t)$ for $H_{FC} = 0.14$ T at different times ($t = t_z$, 10^2, 10^3 and 10^4 s) plotted versus temperature on a logarithmic scale. The slope at $t = t_z$ is -4.7 and that at 10^4 s is -2 (see text).

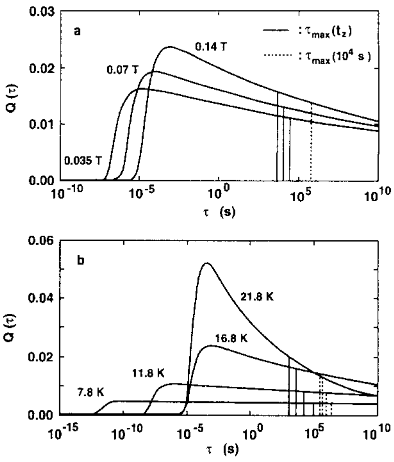

Fig. 10. Variation of the relaxation spectrum $Q(\tau)$ and maximum relaxation time $\tau_{max}(t)$ at $t = t_z$ and 10^4 s with (a) the cooling field H_{FC} at a fixed temperature of 16.8 K and (b) with temperature at a fixed cooling field of $H_{FC} = 0.14$ T.

Moreover, Fig. 10 illustrates the relaxation spectra $Q(\tau)$ for TRM calculated using Eq. (15′) with the obtained parameters t_0 and m, together with the maximum relaxation time $\tau_{max}(t)$ at $t = t_z$ (solid lines) and 10^4 s (broken lines). As shown in Fig. 10a, with increasing cooling field H_{FC}, the lower cutoff t_0 shifts to the longer time side with increased intensity and slope, while the higher cutoff $\tau_{max}(t)$ at $t = t_z$ becomes shorter, but at $t = 10^4$ s it is independent of H_{FC}. The relaxation spectrum depends remarkably on temperature, as shown in Fig. 10b for the typical case of $H_{FC} = 0.14$ T. The lower cutoff shifts to the longer time side with increasing temperature up to 16.8 K, above which it becomes almost constant, and the relaxation spectrum narrows; the upper cutoff also shifts gradually to the shorter time side. These results are in qualitative agreement with those obtained by Nemoto and Takayama [16] from Monte Carlo simulations in the temperature range $0.6 < T/T_g < 2$ for two-dimensional Ising SG, where they assumed that the longer relaxation time represents the dynamical aspect associated with the overturn of the spin cluster to which the spin belongs, while the shorter relaxation time represents the fast

Table 1
Best-fit parameters obtained experimentally of pz and $-2/[(d-2y)p]$, together with the evaluated values p and z using the theoretical values of y for two-dimensional ($d=2$) and three-dimensional ($d=3$) Ising SG by Bray and Moore [12]

d	y	pz	$-2/[(d-2y)p]$	p	z
3	0.19	0.9	−1.5	0.51	1.8
2	−0.29	0.9	−1.5	0.52	1.9

relaxation associated with the local excitation of each spin.

Finally, we evaluated the dynamical parameters for TRM of our SG system. From $t_{\Delta H} \sim H_{FC}^{-1.5}$, we have $-2/[(d-2y)p] = -1.5$ in Eq. (10). With this value, the parameters p and z are evaluated using the theoretical value of y for the two- ($d=2$) and three-dimensional ($d=3$) Ising model of Bray and Moore [12]. Our estimated values are listed in Table 1 ($p \sim 0.5$, $z \sim 2$) together with the theoretical values, and are in good agreement with those estimated by Koper and Hilhorst [6] using the experimental data for insulating SG of $CdCr_{1.7}In_{0.3}S_4$ of Alba et al. [13]. It is of interest to note that the dynamical parameters p and z are independent of the insulating Ising SG or our itinerant magnetic SG.

5. Conclusion

Using the anomalous Hall effect, we have measured the time decay of field-cooled thermoremanent magnetization (TRM) in the spin-glass (SG) phase of itinerant magnetic Fe_xTiS_2 ($x=0.20$, $T_g=41$ K) for cooling field $H_{FC}=0.01$–0.14 T over the time range 10^{-2}–10^4 s with waiting time $t_w = 180$–18000 s below $T/T_g \sim 0.7$. We found the following salient features of the dynamical properties of SG in this material:

(i) In the short time regime $t < t_d$, the time decay of the Hall resistivity (or TRM) after switching off the external field can be expressed in the form of the power law $\rho_H(t) = At^{-m}$, whose exponent m depends on both cooling field H_{FC} and temperature T, while for $t > t_d$ deviations from the power law become appreciable (except for higher field $H_{FC}=0.14$ T at 26.8 K). As found for the cluster-glass (CG; $x=1/4$) phase, the magnetic field and temperature-dependent exponent m is written in the universal form, $m = D\xi^{\gamma}$, where $\xi = 1 - M(t_z)/M^{FC}(T \to 0)$ is a parameter of the 'relative relaxed magnetization' (RRM), with best-fit values of $D=0.30$, $\gamma=1.4$ for $\xi > \xi_C$ ($=0.21$) and $D=2.6$, $\gamma=2.8$ for $\xi < \xi_C$, the γ values being larger than for CG ($\gamma=1.0$).

(ii) Using the 'domain theory' developed by Koper and Hilhorst, numerical calculations were performed for the observed decay curves of TRM over the whole time range with modifications of their theoretical expressions. As a result, we found satisfactory agreement between the simulations and experiments, including the independence of the TRM decay on the waiting time. The minimum relaxation time t_0 in the relaxation spectrum increases with increasing temperature up to 18 K, above which it becomes constant (of the order of 10^{-5}–10^{-7} s), while the upper limit $\tau_{max}(t)$ depends on time, temperature, and cooling field H_{FC}, which is expressed empirically as $\tau_{max}(t) = 3.6 \times 10^4 T^{-2}(1.2 \times 10^4 H_{FC}^{-1.5} T^{-3} + t - t_z)^{0.9}$, which was obtained from the observed parameters t_2^{pz}/t_1 and $t_{\Delta H}$ with the best-fit value of $pz = 0.9$. Using these parameters, the equilibrium relaxation spectra were calculated; the spectra become narrow with increasing temperature and cooing field, which is in qualitative agreement with the Monte Carlo simulations for two-dimensional Ising SG [16].

(iii) Using the dynamical parameters appearing in the domain theory, we can express the parameter of relative relaxed magnetization ξ, which characterizes the temperature and cooling-field dependence of the time decays of TRM in a short time span, in the form $\xi \sim 1 - (t_z/t_0)^{-m}/(-m+1)$, which is a function of t_z/t_0 and the exponent m.

(iv) With the evaluated value $2/[(d-2y)p] = 1.5$ and the theoretical value of y for the two- ($d=2$) and three-dimensional ($d=3$) Ising model, we obtained the dynamical parameters $p \sim 0.5$ (the domain size increases as a power of time with exponent p) and $z \sim 2$ (the upper relaxation time depends on the domain size with exponent z), in agreement with those of some insulating Ising SG. With regard to the nature of magnetism (localized spin or itinerant electron picture), there are no differences in these dynamical parameters. More studies of relaxation phenomena, such as the temperature cycle, are desirable for another viewpoint of the hierarchical kinetics for our itinerant magnetic material.

Acknowledgements

We thank K. Fushimi for his assistance in recording the present data. Part of this work was supported by grants from the Electric Technology Research Foundation of Chugoku, and a grant-in-aid from the Ministry of Education, Science and Culture of Japan.

References

[1] J. Hammann, M. Lederman, M. Ocio, R. Orbach and E. Vincent, Physica A 185 (1992) 278.
[2] F. Lefloch, J. Hammann, M. Ocio and E. Vincent, Europhys. Lett. 18 (1992) 647.
[3] M. Lederman, R. Orbach, J.M. Hammann, M. Ocio and E. Vincent, Phys. Rev. B 44 (1991) 7403.
[4] C.M. Newman and D.L. Stein, Phys. Rev. B 46 (1992) 973.
[5] D.S. Fisher and D.A. Huse, Phys. Rev. Lett. 56 (1986) 1601.
[6] G.J.M. Koper and H.J. Hilhorst, J. Phys. (Paris) 49 (1988) 429.
[7] P. Granberg, L. Lundgren and P. Nordblad, J. Magn. Magn. Mater. 92 (1990) 228.
[8] Y. Hara, W.X. Gao, H. Negishi and M. Inoue, J. Magn. Magn. Mater. 135 (1994) 311.
[9] Y. Hara, H. Negishi, M. Sasaki, M. Inoue and V.A. Kulbachinskii, J. Magn. Magn. Mater. 145 (1995) 157.
[10] N. Bontemps and R. Orbach, Phys. Rev. B 37 (1988) 4708.
[11] M. Inoue, K. Sadahiro and H. Negishi, J. Magn. Magn. Mater. 98 (1991) 60.
[12] A.J. Bray and M.A. Moore, Phys. Rev. Lett. 58 (1987) 57.
[13] M. Alba, E. Vincent, J. Hammann and M. Ocio, J. Appl. Phys. 61 (1987) 4092.
[14] A.T. Ogielski, Phys. Rev B 32 (1985) 7384.
[15] A. Ito, H. Aruga, E. Torikai, M. Kikuchi, Y. Syono and H. Takei, Phys. Rev. Lett. 57 (1986) 483.
[16] K. Nemoto and H. Takayama, J. Phys. C 16 (1983) 6835.